Struct Multidisc Optim (2012) 45:657–668
DOI 10.1007/s00158-011-0715-y

RESEARCH PAPER

Minmax topology optimization

Kevin Brittain · Mariana Silva · Daniel A. Tortorelli

Received: 23 May 2011 / Revised: 30 August 2011 / Accepted: 7 September 2011 / Published online: 12 October 2011

Abstract We describe a systematic approach for the robust optimal design of linear elastic structures subjected to unknown loading using minmax and topology optimization methods. Assuming only the loading region and norm, we distribute a given amount of material in the design domain to minimize the *principal compliance*, i.e. the maximum compliance that is produced by the worst-case loading scenario. We evaluate the principal compliance directly by satisfying the optimality conditions which take the form of a Steklov eigenvalue problem and thus we eliminate the need of an iterative nested optimization. To generate a well-posed topology optimization problem we use relaxation which requires homogenization theory. Examples are provided to demonstrate our algorithm.

Keywords Topology optimization · Homogenization · Robust design

1 Introduction

Traditionally when solving a topology optimization problem, the external loads are deterministic (Bendsøe and Sigmund 2003). As such the resulting optimal designs are vulnerable to slight loading variations. An extreme example is a cantilever beam that is designed for a pure tension load and then subjected to a bending load. The beam clearly performs poorly when subjected to the latter loading.

K. Brittain (✉) · M. Silva · D. A. Tortorelli
Department of Mechanical Science and Engineering,
University of Illinois at Urbana-Champaign,
1206 West Green St., Urbana, IL 61801, USA
e-mail: kevin.brittain7@gmail.com

Fortunately topology design of structures subject to uncertain loadings has recently received significant attention. Díaz and Bendsøe (1992) generate robust designs by subjecting structures to multiple load cases. In their formulation they minimize the norm of a set of weighted compliances resulting from the individual load cases. This work is extended in Guest and Igusa (2008) to include loads characterized by continuous joint probability density functions and to account for uncertainties in structural geometry. Reliability-based topology optimization (RBTO) methods are also utilized to design structures for uncertainties by assuming stochastic distributions of the model parameter (Kharmanda et al. 2004). Silva et al. (2010) consider a Gaussian distribution of the applied loads while Jung and Cho (2004) consider material properties. Typical RBTO algorithms require nested optimizations; the outer problem optimizes the design variables while the inner problem optimizes the stochastic model parameters. Methods to eliminate the iterative solution of the inner problem appear in Silva et al. (2010). For further developments in RBTO, see Maute and Frangopol (2003), Allen and Maute (2005) and Mozumder et al. (2006). Robust topology optimization (RTO) is similar to RBTO, wherein response functions are replaced by the sum of their mean values and their weighted variances, cf. Kogiso et al. (2008). RTO is also used to design structures for random field uncertainties in loading and material properties by combining shape and topology optimization with Karhunen-Loeve expansions, cf. Conti et al. (2009) and Chen et al. (2010). Other robust design alternatives are available, like the sensitivity-based formulations in Sundaresan et al. (1995) and Kogiso et al. (2008). An overview of still other robust design approaches such as the Taguchi method, physical programming approach, and robust design with an axiomatic approach are discussed in Park et al. (2006).

Another way to accommodate uncertain loadings is to solve a minmax design problem. For example in Cherkaev and Cherkaev (2003, 2008), a structure is optimized to minimize the *principal compliance*, i.e. the maximum compliance that is produced by the worst-case loading subject to a net load norm constraint. As with RBTO, the minmax problem is also characterized by nested outer and inner optimization problems. More recently this minmax formulation was applied to topology optimization using the restriction method and SIMP (Takezawa et al. 2011); the analyzes only consider point loadings. An interesting variation to the minmax problem is discussed by Cherkaev and Cherkaev (2003) and Gournay et al. (2008) wherein a nominal load is applied to the structure. The minmax problem then considers the worst-case load perturbation, rather than the net load.

Minmax structural design problems also appear in Olhoff (1989) and Bendsøe et al. (1983) where the maximum of a set of weighted cost functions is minimized. In these works the minmax problem is reformulated into the so-called "bound formulation" to alleviate the non-differentiability issues that would otherwise arise, and hence making the bound formulation amendable to traditional nonlinear programming algorithms. As an example, this formulation is used to design a simply supported beam to minimize the maximum of compliance and deflection subject to resource constraints (Bendsøe et al. 1983); no load variability is considered.

Herein, we use minmax and topology optimization methods to generate robust designs by optimizing a structure's material distribution subject to a resource constraint. Only the loading region and norm are assigned; its distribution is otherwise random and we select its worst-case realization. As previously stated, two optimizations are required to solve minmax problems. In our outer loop we distribute a given amount of material by using a material distribution topology formulation and in the inner loop we determine the worst-case loading. As in reliability methods, cf. Silva et al. (2010), the inner loop is often solved using iterative nonlinear programming techniques. However, we solve the inner loop directly by satisfying the Karush Kuhn Tucker (KKT) optimality conditions which take the form of an eigenvalue problem, cf. Cherkaev and Cherkaev (2008) and thus we significantly reduce the computation time.

The remainder of this paper is organized as follows. In Section 2.1 we discuss the governing equations for our linear elastostatic structure. We introduce the sequentially-ranked laminate material model in Section 2.2 and formulate the minmax optimization problem in Section 2.3. The nested optimization problem is solved by using an optimality criteria based algorithm to update the microstructure design parameters and an eigenvalue problem to evaluate the worst-case loading as described in Section 2.4. We present representative example designs produced using the minmax optimization formulation in Section 2.5 and we draw conclusions in Section 3. The finite element discretization appears in the Appendix.

2 Material design using minmax formulation

2.1 Linear elastostatic system

In topology optimization two or more material phases are optimally distributed to maximize structural performance, cf. Bendsøe and Sigmund (2003). To make the problem well-posed restriction can be used to limit the oscillations between the phases, cf. Bendsøe (1989), or relaxation can be used to incorporate the infinitesimal oscillations via homogenization theory, cf. Allaire (2002). We use relaxation. And hence at each location in the domain, the volume fraction of each material phase is specified, and the microstructure is prescribed to produce the optimal effective properties so as to minimize the cost function and satisfy the constraints. This set of all obtainable effective properties for the given phase volume fractions is the $\mathcal{G}$-closure and thus for the given phase volume fractions we prescribe the optimal microstructure from the $\mathcal{G}$-closure. Unfortunately, the $\mathcal{G}$-closure is unknown so we use a partial relaxation and design with sequentially-ranked laminates which are known to be optimal for compliance designs (Allaire 2002). Moreover explicit formulae are available to obtain the effective properties, cf. Allaire (2002). And hence the microstructure fields that describe the sequentially-ranked laminates are readily optimized.

Our structure is comprised of a two-phase sequentially-ranked laminate composite such that each material point in the design domain, Ω, is defined by an anisotropic heterogeneous unit cell, cf. Fig. 1. The boundary of the domain, $\partial\Omega$, is divided into three complementary regions: Γ_N on which the worst-case tractions are prescribed, Γ_0 on which homogeneous Neumann boundary conditions are prescribed

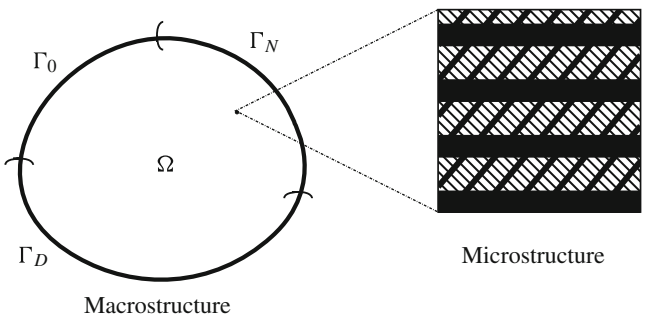

Fig. 1 Design domain

and Γ_D on which homogeneous Dirichlet boundary conditions are prescribed. We assume the structure adheres to the governing equations of linear elastostatics

$$\begin{aligned} \operatorname{div}(\mathbb{C}[\nabla \mathbf{u}]) &= \mathbf{0} \quad \text{in} \quad \Omega \\ (\mathbb{C}[\nabla \mathbf{u}])\,\mathbf{n} &= \mathbf{t} \quad \text{on} \quad \Gamma_N \\ (\mathbb{C}[\nabla \mathbf{u}])\,\mathbf{n} &= \mathbf{0} \quad \text{on} \quad \Gamma_0 \\ \mathbf{u} &= \mathbf{0} \quad \text{on} \quad \Gamma_D \end{aligned} \tag{1}$$

where $\mathbf{u}$ is the displacement, $\mathbb{C}$ is the material elasticity tensor and $\mathbf{t}$ is the applied traction. Note that we assume no body loads.

In the weak formulation of the above problem we are to find the displacement $\mathbf{u} \in \mathcal{U} = \{\mathbf{u} \in H^1(\Omega) \mid \mathbf{u} = \mathbf{0} \text{ on } \Gamma_D\}$ that satisfies the residual equation

$$r(\mathbf{w}; \mathbf{u}) = \int_\Omega \nabla \mathbf{w} \cdot \mathbb{C}[\nabla \mathbf{u}]\, d\Omega - \int_{\Gamma_N} \mathbf{w} \cdot \mathbf{t}\, d\Gamma = 0 \tag{2}$$

for all $\mathbf{w} \in \mathcal{U}$, where $\mathbf{w}$ is the weighting function.

Utilizing the homogenization theory presented in Allaire (2002) we take the elastostatic formulation and replace it by a homogenized ("averaged") form which uses the averaged displacement, $\mathbf{u}_0$, and homogenized material elasticity tensor, $\mathbb{C}^h$. We are not interested in recovering the point-wise, i.e. local, responses in the microstructure therefore the averaged displacement suffices. For conciseness, we omit the index "0" of the averaged displacement, i.e. the averaged displacement is here and henceforth denoted by $\mathbf{u}$.

2.2 Sequentially-ranked laminates

As mentioned above, we use relaxation to make our topology optimization well-posed. And since the $\mathcal{G}$-closure is unknown we use a partial relaxation by designing with sequentially-ranked laminates. Moreover we use rank-3 laminates since the homogenized properties for rank-N with $N > 3$ can be obtained by a rank-3 laminate in two-dimensions, cf. Allaire (2002).

The sequentially ranked-laminate, cf. Allaire (2002), Le et al. (2011), is constructed by sequentially laminating two materials: the reinforcement and matrix with elasticity tensors $\mathbb{C}^+$ and $\mathbb{C}^-$ as follows. A rank-1 laminate is formed by layering the two materials as depicted in Fig. 2. The reinforcement volume fraction, ρ_1, and the layer orientation, φ_1, are the two parameters that describe this microstructure. A rank-2 laminate is formed by using the rank-1 laminate as the matrix and layering the reinforcement material using analogous parameters ρ_2 and φ_2. Similarly, a rank-3 laminate is formed by layering a third layer of reinforcement material on the rank-2 laminate via the parameters ρ_3 and φ_3.

The homogenized elasticity tensor $\mathbb{C}^h$ for a sequentially-ranked laminate is derived analytically in Allaire (2002). If the base materials are isotropic, the formula for the homogenized rank-N elasticity tensor $\mathbb{C}^h$, cf. (2.69) in Allaire (2002) is:

$$(1-\rho)\left(\mathbb{C}^h - \mathbb{C}^-\right)^{-1} = \left(\mathbb{C}^+ - \mathbb{C}^-\right)^{-1} + \rho \sum_{i=1}^{N} m_i\, \mathbb{F}^-(\mathbf{e}_i) \tag{3}$$

where the $\mathbf{e}_i$ are the lamination orientations, ρ is the total volume fraction of the reinforcement material

$$\rho(\mathbf{d}) = 1 - \prod_{i=1}^{N} (1-\rho_i) \tag{4}$$

and the m_i are the volume fraction-like parameters satisfying

$$m_i(\mathbf{d}) = \frac{\rho_i}{\rho(\mathbf{d})} \prod_{j=1}^{i-1} (1-\rho_j) \quad i = 1, \ldots, N-1 \tag{5}$$

and

$$\sum_{i=1}^{N} m_i(\mathbf{d}) = 1 \;\text{ and }\; m_i(\mathbf{d}) \geq 0 \tag{6}$$

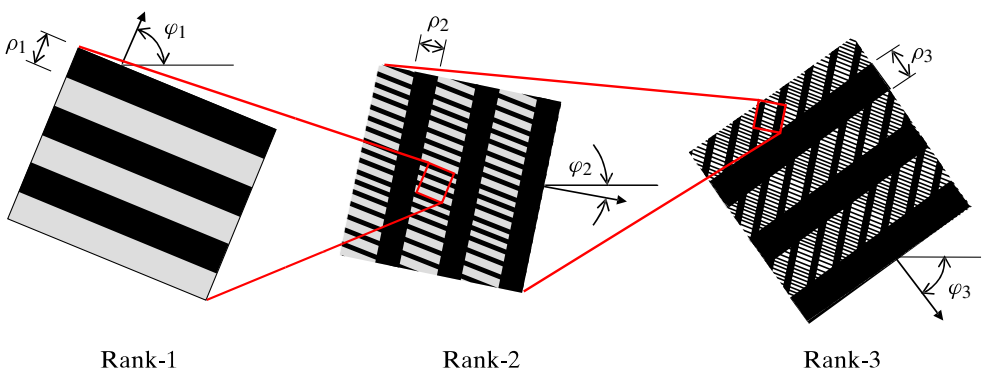

Fig. 2 Sequentially-ranked laminate, cf. Le et al. (2011)

therefore we require

$$m_N(\mathbf{d}) = 1 - \sum_{i=1}^{N-1} m_i(\mathbf{d}) \tag{7}$$

The vector $\mathbf{d} = [\rho_1, \rho_2, \rho_3, \varphi_1, \varphi_2, \varphi_3]^T$ describes the laminate field; it is optimized. $\mathbb{F}^-(\mathbf{e})$ is a fourth-order tensor with major and minor symmetries defined by

$$\mathbb{F}^-(\mathbf{e}) = \frac{1}{\mu^-}\left(\mathbb{S}(\mathbf{e}\otimes\mathbf{e}) - (\mathbf{e}\otimes\mathbf{e})\otimes(\mathbf{e}\otimes\mathbf{e})\right) + \frac{1}{2\mu^- + \lambda^-}(\mathbf{e}\otimes\mathbf{e})\otimes(\mathbf{e}\otimes\mathbf{e}) \tag{8}$$

where $\mathbb{S}$ is a fourth-order symmetrizer and in two-dimensions $\mathbf{e} = \{e_1, e_2\}^T$ so that $\mathbf{e}_i(\mathbf{d}) = \{\cos\varphi_i, \sin\varphi_i\}^T$.

The sensitivity of the homogenized elasticity tensor, $\mathbb{C}^h$, with respect to the sequentially-ranked laminate design field, $\mathbf{d}$, is required for the optimization. To compute the sensitivity of $\mathbb{C}^h$, as shown by Le et al. (2011), we rewrite (3) as:

$$\mathbb{C}^h(\mathbf{d}) = (1 - \rho(\mathbf{d}))\,\mathbb{D}^{-1}(\mathbf{d}) + \mathbb{C}^- \tag{9}$$

where

$$\mathbb{D}(\mathbf{d}) = (\mathbb{C}^+ - \mathbb{C}^-)^{-1} + \rho(\mathbf{d})\sum_{i=1}^{N} m_i(\mathbf{d})\,\mathbb{F}^-(\mathbf{e}_i(\mathbf{d})) \tag{10}$$

The derivative of the above with respect to ρ_i is obtained by first noting that

$$\frac{\partial\mathbb{C}^h}{\partial\rho} = -\mathbb{D}^{-1} - (1-\rho)\,\mathbb{D}^{-1}\left[\sum_{i=1}^{N} m_i\,\mathbb{F}^-(\mathbf{e}_i(\varphi_i))\right]\mathbb{D}^{-1} \tag{11}$$

$$\frac{\partial\mathbb{C}^h}{\partial m_j} = -\rho\,(1-\rho)\,\mathbb{D}^{-1}\,\mathbb{F}^-(\mathbf{e}_j(\varphi_j))\,\mathbb{D}^{-1} \tag{12}$$

Derivatives with respect to ρ_i are then obtained by differentiating (4) and (5) and applying the chain-rule to (11) and (12) i.e.

$$\frac{D\rho}{D\rho_i} = \prod_{\substack{j=1\\ j\neq i}}^{N}(1-\rho_j) \tag{13}$$

$$\frac{Dm_j}{D\rho_i} = \frac{\partial m_j}{\partial\rho}\frac{\partial\rho}{\partial\rho_i} + \frac{\partial m_j}{\partial\rho_i} \quad j = 1, ..., N-1 \tag{14}$$

where

$$\frac{\partial m_j}{\partial\rho} = -\frac{\rho_j}{\rho^2}\prod_{i=1}^{j-1}(1-\rho_i) \tag{15}$$

and

$$\frac{\partial m_j}{\partial\rho_i} = \frac{1}{\rho}\left[\delta_{ij}\prod_{i=1}^{j-1}(1-\rho_i) - \rho_j\prod_{\substack{k=1\\ k\neq i}}^{j-1}(1-\rho_k)\right] \tag{16}$$

where $j = 1, ..., N-1$ and

$$\frac{Dm_N}{D\rho_i} = -\sum_{j=1}^{N-1}\frac{\partial m_j}{\partial\rho_i} \tag{17}$$

The derivatives with respect to the φ_i are computed directly as

$$\frac{\partial\mathbb{C}^h}{\partial\varphi_i} = -\rho(1-\rho)m_i\,\mathbb{D}^{-1}\frac{\partial\mathbb{F}^-(\mathbf{e}_i(\varphi_i))}{\partial\varphi_i}\,\mathbb{D}^{-1} \tag{18}$$

2.3 Minmax formulation

The principal compliance, Λ, is defined as the compliance corresponding to the worst-case loading scenario i.e.

$$\Lambda\left(\mathbb{C}^h\right) = \max_{\mathbf{t}\in\mathcal{F}}\ \beta\left(\mathbf{t}, \mathbb{C}^h\right) \tag{19}$$

$$\text{such that: } \phi(\mathbf{t}) = \int_{\Gamma_N}\mathbf{t}\cdot\mathbf{t}\,d\Gamma - \bar{t}^2 = 0$$

where $\mathcal{F}$ is the set of admissible, i.e. smooth, functions on Γ_N, ϕ is the constraint function on the traction norm which we limit to $\bar{t}$ and the cost function is the compliance i.e.

$$\beta\left(\mathbf{t}, \mathbb{C}^h\right) = \int_{\Gamma_N}\mathbf{u}\cdot\mathbf{t}\,d\Gamma \tag{20}$$

Since the displacement, $\mathbf{u}$, is a function of the homogenized elasticity tensor, $\mathbb{C}^h$, and the traction, $\mathbf{t}$, β is implicitly defined by $\mathbb{C}^h$ and $\mathbf{t}$ via the governing field equations of linear elastostatics cf (1).

To generate the robust design we minimize the principal compliance of the structure. The resulting minmax topology optimization problem is expressed as

$$\min_{\mathbf{d}\in\mathcal{H}}\ \Lambda\left(\mathbb{C}^h(\mathbf{d})\right) \tag{21}$$

$$\text{such that: } \alpha(\mathbf{d}) = V(\rho(\mathbf{d})) - \bar{V} \leq 0$$

where $\mathcal{H}$ is the set of admissible, not necessarily smooth functions on Ω. As seen above we limit the volume of reinforcement material $V(\rho) = \int_\Omega \rho\,dv$ to $\bar{V}$.

It is clear that two distinct optimizations must be solved in this minmax formulation, i.e. the compliance, β, must be maximized with respect to the traction, $\mathbf{t}$, and minimized with respect to the laminate design parameters, $\mathbf{d}$.

To solve the inner and outer loops we require sensitivities of the cost function and constraint functions with respect to the traction, $\mathbf{t}$, and laminate design parameters, $\mathbf{d}$. Toward this end we note that the variation of β with respect to $\mathbf{t}$ is obtained using the usual adjoint method, cf. Tortorelli and Michaleris (1994), i.e.

$$\delta\beta\left(\mathbf{t}, \mathbb{C}^h; \delta\mathbf{t}\right) = 2\int_{\Gamma_N} \mathbf{u}\cdot\delta\mathbf{t}\, d\Gamma \tag{22}$$

Of course if we change the material, i.e. $\mathbb{C}^h$, we will get a different worst-case traction, $\mathbf{t}^*$, therefore the worst-case traction, $\mathbf{t}^*$, is a function of the homogenized elasticity tensor, $\mathbb{C}^h$, i.e. $\mathbf{t}^*(\mathbb{C}^h)$. To account for this dependence in the outer problem we write the Lagrangian of the inner problem and recognize that, at worst-case traction, $\mathbf{t}^*$, the Lagrangian equals the principal compliance, i.e.

$$\begin{aligned} L\left(\mathbf{t}^*(\mathbb{C}^h\right), \lambda^*\left(\mathbb{C}^h\right), \mathbb{C}^h\right) &= \Lambda\left(\mathbb{C}^h\right) \\ &= \beta\left(\mathbf{t}^*\left(\mathbb{C}^h\right), \mathbb{C}^h\right) + \lambda^*\left(\mathbb{C}^h\right)\phi\left(\mathbf{t}^*\left(\mathbb{C}^h\right)\right) \end{aligned} \tag{23}$$

where λ^* is the value of the Lagrange multiplier at the optimum; it is also a function of $\mathbb{C}^h$. Returning to the outer problem we see that the variation of the principal compliance, Λ, with respect to the elasticity tensor, $\mathbb{C}^h$, is

$$\begin{aligned} \delta L\left(\mathbf{t}^*\left(\mathbb{C}^h\right), \mathbb{C}^h; \delta\mathbb{C}^h\right) = \Big[&\delta\beta\left(\mathbf{t}^*\left(\mathbb{C}^h\right), \mathbb{C}^h; \delta\mathbf{t}^*\left(\mathbb{C}^h; \delta\mathbb{C}^h\right)\right) \\ &+ \lambda^*\left(\mathbb{C}^h\right)\delta\phi\left(\mathbf{t}^*\left(\mathbb{C}^h\right); \delta\mathbf{t}^*\left(\mathbb{C}^h; \delta\mathbb{C}^h\right)\right) \\ &+ \delta\lambda^*\left(\mathbb{C}^h; \delta\mathbb{C}^h\right)\phi\left(\mathbf{t}^*\left(\mathbb{C}^h\right)\right)\Big] \\ &+ \delta\beta\left(\mathbf{t}^*\left(\mathbb{C}^h\right), \mathbb{C}^h; \delta\mathbb{C}^h\right) \end{aligned} \tag{24}$$

which implies

$$\delta\Lambda\left(\mathbb{C}^h; \delta\mathbb{C}^h\right) = \delta\beta\left(\mathbf{t}^*\left(\mathbb{C}^h\right), \mathbb{C}^h; \delta\mathbb{C}^h\right) \tag{25}$$

since the term in brackets equals zero as a result of the inner problem optimality condition. This reveals that the dependence of the traction on the material distribution can be neglected when computing the sensitivity of Λ and hence

$$\delta\Lambda\left(\mathbb{C}^h; \delta\mathbb{C}^h\right) = -\int_\Omega \nabla\mathbf{u}\cdot\delta\mathbb{C}^h[\nabla\mathbf{u}]\, dv \tag{26}$$

which follows from the adjoint method. To obtain the variation of Λ with respect to $\delta\mathbf{d}$, we use the above variation with respect to $\delta\mathbb{C}^h$ and (11)–(18).

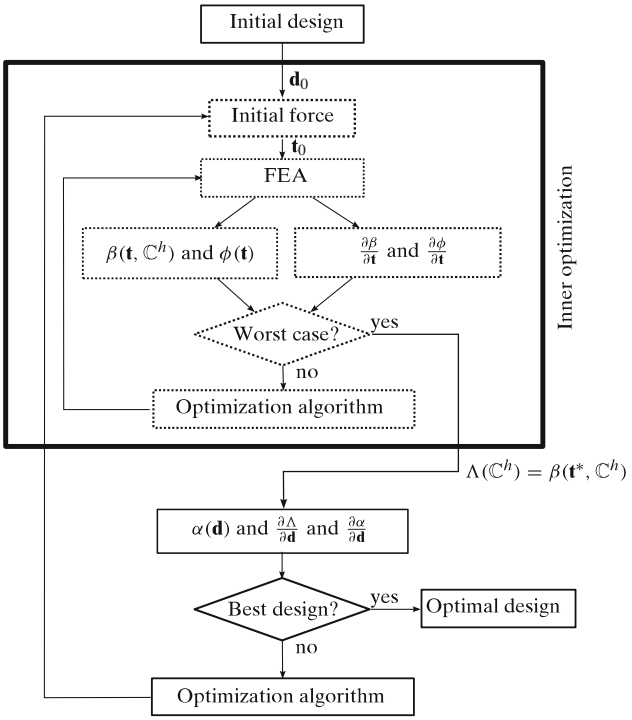

Fig. 3 Minmax optimization flowchart

2.4 Nested optimization formulation

Nonlinear programming can be utilized to solve the inner loading optimization problem. For each iteration the outer minimization generates a new material distribution, $\mathbb{C}^h$, and the inner optimization loop is solved to maximize the compliance with respect to the loading, $\mathbf{t}$. A flow chart of the minmax optimization problem with the inner optimization loop appears in Fig. 3. To solve the inner optimization we could use the adjoint method to compute the sensitivity[1] and an optimizer such as the Most Probable Point of Inverse Reliability (MPPIR) search algorithm defined in Du et al. (2004) to iteratively update the load, $\mathbf{t}$. Although the MPPIR search algorithm reaches the maximum quickly and efficiently, the many solutions of the inner loop for each material distribution design iteration is nonetheless computationally costly.

2.4.1 Analytical inner loop algorithm

It is clear that the inner optimization problem can be costly to solve. In order to reduce this expense, we replace the iterative solution of the inner problem by an analytical computation cf. Cherkaev and Cherkaev (2008). Indeed

[1]The sensitivity is computed after the appropriate finite element discretization, see the Appendix for details.

using optimality conditions we develop a Steklov eigenvalue problem, whose dominate eigenvalue provides the worst-case compliance.

To begin we express the Lagrangian of the inner problem as

$$L(\mathbf{t}, \lambda) = \beta(\mathbf{t}) - \lambda\left(\int_{\Gamma_N} \mathbf{t}\cdot\mathbf{t}\, d\Gamma - \bar{t}^2\right) \tag{27}$$

where λ is the Lagrange multiplier, cf. (23). In this inner problem $\mathbb{C}^h$ is fixed and hence we omit its argument.

The variation of the Lagrangian requires the variation of β with respect to the traction, $\mathbf{t}$, which we obtain via the adjoint method (Cherkaev and Cherkaev 2008), cf. (22), and thus

$$\begin{aligned}\delta L(\mathbf{t}, \lambda; \delta\mathbf{t}) &= \delta\beta(\mathbf{t}; \delta\mathbf{t}) - \lambda \int_{\Gamma_N} 2\,\mathbf{t}\cdot\delta\mathbf{t}\, d\Gamma \\ &= \int_{\Gamma_N} (2\,\mathbf{u} - 2\,\lambda\,\mathbf{t})\cdot\delta\mathbf{t}\, d\Gamma \end{aligned} \tag{28}$$

The optimality condition $\delta L(\mathbf{t}, \lambda; \delta\mathbf{t}) = 0$ and a localization argument lead to

$$\mathbf{t} = \frac{\mathbf{u}}{\lambda} \quad \text{on } \Gamma_N \tag{29}$$

i.e. the worst-case loading satisfies $\mathbf{t}^* = 1/\lambda^*\,\mathbf{u}$.

Using this traction the residual equation for the weak linear elastostatics formulation (2) becomes

$$\begin{aligned} r(\mathbf{w}; \mathbf{u}) = &\int_\Omega \nabla\mathbf{w}\cdot\mathbb{C}^h[\nabla\mathbf{u}]\, d\Omega \\ &- \int_{\Gamma_N} \mathbf{w}\cdot\overbrace{\frac{1}{\lambda^*}\mathbf{u}}^{=\mathbf{t}^*}\, d\Gamma = 0 \end{aligned} \tag{30}$$

Due to the existence of $\mathbf{u}$ in both the energy bilinear and load linear forms, the weak formulation takes the form of a Steklov eigenvalue problem which we solve for the eigenpairs $(\lambda, \mathbf{u})$.[2]

The eigenpairs $(\lambda, \mathbf{u})$ can be used to compute the principal compliance. Indeed we use (29) to obtain $\mathbf{u} = \lambda^*\,\mathbf{t}^*$ on Γ_N. Substituting this relationship into (20) subsequently yields

$$\beta(\mathbf{t}^*) = \lambda^* \int_{\Gamma_N} \mathbf{t}^*\cdot\mathbf{t}^*\, d\Gamma = \lambda^*\,\bar{t}^2 \tag{31}$$

where we also use the constraint in (19). Evidently the worst-case compliance for the given material distribution, $\mathbb{C}^h$, corresponds to the dominant eigenvalue, i.e. $\lambda^* = \lambda_{\max}$ and thusly

$$\Lambda = \lambda_{\max}\,\bar{t}^2 \tag{32}$$

As seen here, we replaced the iterative solution of the inner problem with an eigenvalue analysis.

In regard to (25) we note that the variation of the principal compliance is expressed as

$$\delta\Lambda(\mathbb{C}^h; \delta\mathbb{C}^h) = \delta\lambda_{\max}(\mathbb{C}^h; \delta\mathbb{C}^h)\,\bar{t}^2 \tag{33}$$

where the eigenvalue variation is obtained by the methods described in Seyranian et al. (1994). Of course, this equation is only true for simple eigenvalues as repeated eigenvalues are nondifferentiable, although they do have directional derivatives, cf. Courant and Hilbert (1953) and Seyranian et al. (1994). Fortunately, we do not encounter repeated eigenvalues in our examples. However, they have been encountered in minmax problems, cf. Gournay et al. (2008) and Cherkaev and Cherkaev (2003, 2008).

Note that we never actually solve the equilibrium equation. Indeed, any eigenvalue, eigenvector pair solves (30). We select the pair that corresponds to the maximum eigenvalue, i.e. $(\lambda_{\max}, \mathbf{u}^{\max})$. Being that as it may, any scalar multiple, $\bar{\mathbf{u}} = \alpha\,\mathbf{u}^{\max}$, also satisfies (30). To these ends, we scale $\mathbf{u}^{\max}$ such that the constraint of (19) is satisfied, i.e. we find α that satisfies

$$\int_{\Gamma_N} \mathbf{t}^*\cdot\mathbf{t}^*\, d\Gamma = \frac{\alpha^2}{\lambda_{\max}^2}\int_{\Gamma_N} \mathbf{u}^{\max}\cdot\mathbf{u}^{\max}\, d\Gamma = \bar{t}^2 \tag{34}$$

where we use $\mathbf{t}^* = 1/\lambda_{\max}\,\bar{\mathbf{u}}$, cf. (29), and the scaled displacement $\bar{\mathbf{u}}$ which defines the structural deformation under the worst-case loading with norm $\bar{t}$.

The constraint on the force uses the L_2 norm and as expected our results would vary if we select another norm. For example, if we use the L_1 norm, i.e. $\phi(\mathbf{t}) = \int_{\Gamma_N} \sqrt{\mathbf{t}\cdot\mathbf{t}}\, d\Gamma - \bar{t} = 0$ then we would replace (29) with $\mathbf{t}/\sqrt{\mathbf{t}\cdot\mathbf{t}} = 2\,\mathbf{u}\,\lambda$ on Γ_N which implies $|\mathbf{u}| = \lambda/2$ is uniform over Γ_N. And hence if Γ_N abuts Γ_D then we would not be able to apply homogeneous Dirichlet conditions, lest we would violate smoothness requirements. As discussed in Cherkaev and Cherkaev (2003) this problem is resolved by treating the loading as a distribution which leads to the appearance of concentrated worst-case loads.

2.4.2 *Optimality criteria based outer algorithm*

In order to update the laminate design parameters in the outer loop cf. (21), we use the optimality criteria algorithm described in Bendsøe and Sigmund (2003) due to its simplicity and effectiveness for single constraint problems

[2] As seen in (30) and (41), we are not following the usual convention in which we solve the problem $(\mathbf{K} - \lambda\,\mathbf{M})\,\boldsymbol{\phi} = \mathbf{0}$ rather we use the "reciprocal" eigenvalue and solve $(\lambda\,\mathbf{K} - \mathbf{M})\,\boldsymbol{\phi} = \mathbf{0}$.

like ours. The element k laminate orientations, φ_i^k are updated via

$$
\begin{aligned}
D &= \frac{\partial \Lambda}{\partial \varphi_i^k} \\
\varsigma &= -s_i^{\varphi^k} \operatorname{sign}(D)|D|^\eta \\
\Delta\varphi_i^k &= \max\{\upsilon^{\varphi-}, \min\{\upsilon^{\varphi+}, \varsigma\}\} \\
\varphi_i^k &= \varphi_i^k + \Delta\varphi_i^k
\end{aligned} \tag{35}
$$

where η is a control parameter that is usually equated to 0.5, $\upsilon^{\varphi+}$ and $\upsilon^{\varphi-}$ are the upper and lower move limits and the $s_i^{\varphi^k}$ are scaling factors which are updated each optimization iteration based on whether the value of φ_i^k oscillates between successive iterations or not, cf. Svanberg (1987). The element k volume fractions, ρ_i^k, are similarly updated via

$$
\begin{aligned}
D &= \frac{\partial \Lambda}{\partial \rho_i^k} \Big/ \frac{\partial \phi}{\partial \rho_i^k} - \Lambda^o \\
\varsigma &= -s_i^{\rho^k} \operatorname{sign}(D)|D|^\eta \\
\Delta\rho_i^k &= \max\{\upsilon^{\rho-}, \min\{\upsilon^{\rho+}, \varsigma\}\} \\
\rho_i^k &= \rho_i^k + \Delta\rho_i^k
\end{aligned} \tag{36}
$$

where $\upsilon^{\rho+}$ and $\upsilon^{\rho-}$ are the upper and lower move limits and Λ^o is the Lagrange multiplier-like term computed, e.g. using the bi-section method, such that the updated design satisfies the volume constraint $\alpha(\mathbf{d}) = 0$ (Bendsøe and Sigmund 2003).

2.5 Numerical examples

In the following examples, we optimize the microstructures of plane strain structures to minimize the principal compliance subject to a constraint that the isotropic reinforcement

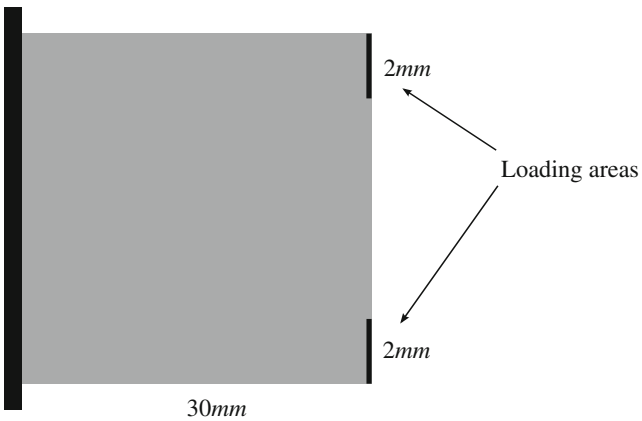

Fig. 4 Square cantilever beam design space and loading areas

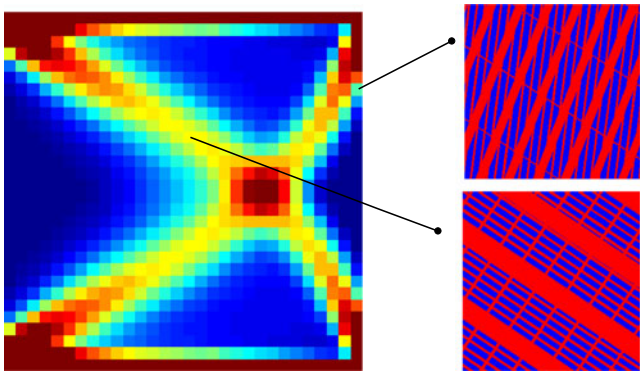

Fig. 5 Optimized cantilever beam design (volume fraction ρ) for the minimum principal compliance problem obtained with a 30×30 mesh. The highlighted elements illustrate the ranked-laminate microstructure

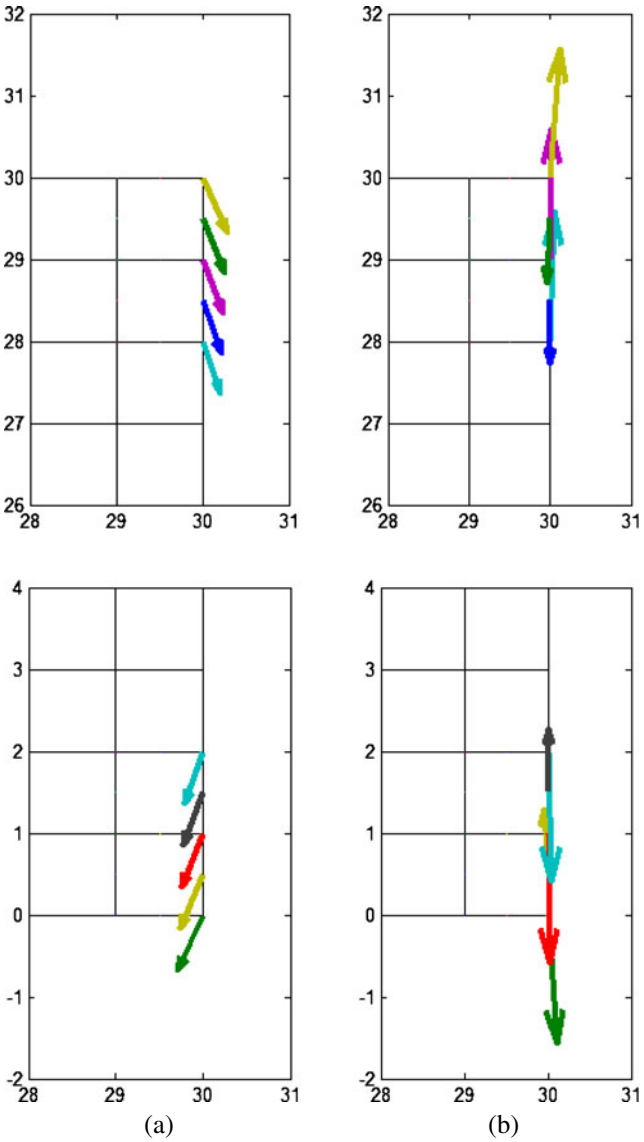

Fig. 6 Optimized loads for a 30×30 mesh: **a** Worst case loading on the top and bottom loading areas; **b** Best-case loading on the top and bottom loading areas

material (with Young's modulus 100 times greater than the isotropic matrix material) can fill no more than 40% of the design domain. We discretize our domain by employing finite elements. The applied traction $\mathbf{t}$ is parameterized by the usual finite element shape functions and node loads, whereby each node in the loading region is assigned a force in the two coordinate directions. The collection of these parameters defines the load parameter vector. The prescribed traction loading norm is $\bar{t}^2 = 2.0$. The field $\mathbf{d}$ is replaced by a piecewise uniform representation whereby each finite element k in the domain is assigned its own set of laminate parameters, $\mathbf{d}_k$; the collection of these parameters defines the design parameter vector. Babuska-Brezzi like numerical instabilities often cause numerical instabilities in topology optimization problems like the ones we present. In order to resolve these instabilities we use quadratic 8-node (Q8) quadrilateral elements, cf. Díaz and Sigmund (1995); Jog and Haber (1996). In both examples, the loading region and norm are the only load characteristics prescribed.

2.5.1 *Square cantilever*

In the first example, we design a square cantilever beam subjected to two load areas at the extremes of the right-most boundary, cf. Fig. 4. Due to the symmetric characteristic of this problem, we assign the design parameter vector $\mathbf{d}_k$ to the finite elements k at the bottom half of the domain (master elements). The finite elements at the top of the domain (slave) are mapped into the bottom ones such that the final design is symmetric. This assignment is not only for convenience but it also serves to satisfy the symmetry requirements discussed in Theorem 6 of Cherkaev and Cherkaev (2003).

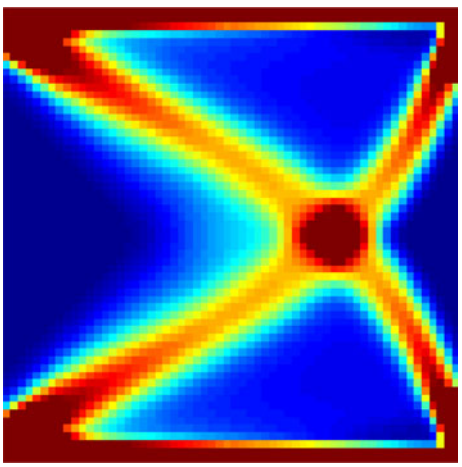

Fig. 7 Optimized cantilever beam design (volume fraction ρ) for the minimum principal compliance problem obtained with a 60×60 mesh

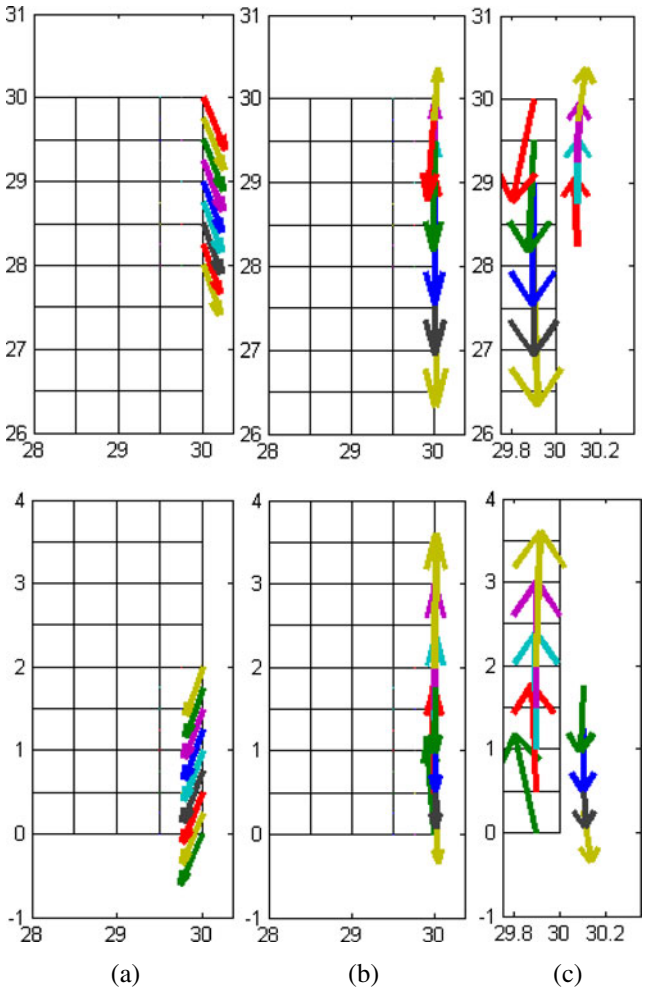

Fig. 8 Optimized loads for a 60×60 mesh: (**a**) Worst-case loading on the top and bottom loading areas; (**b**) Best-case loading on the top and bottom loading areas; (**c**) Nodal loads are offset for better visualization

Figure 5 shows the optimized symmetric design for the worst-case loading using a 30×30 mesh. The red to blue represents the variation of the volume fractions ρ for the strong-expensive reinforcement to the weak-inexpensive matrix phases in the volume fraction plots as well as the laminate configuration in the microstructure plot. The highlighted microstructures illustrate that the optimized design contains rank 3 laminates which are known to be optimal for multi-load case compliance optimization problems

Table 1 Compliance comparison of square cantilever beam

Load case	Compliance (30×30 mesh)	Compliance (60×60 mesh)
Worst case	1.5335	1.5134
Tension	0.6237	0.6244
Bending	1.0256	1.0115
Best-case	.00089	.00042

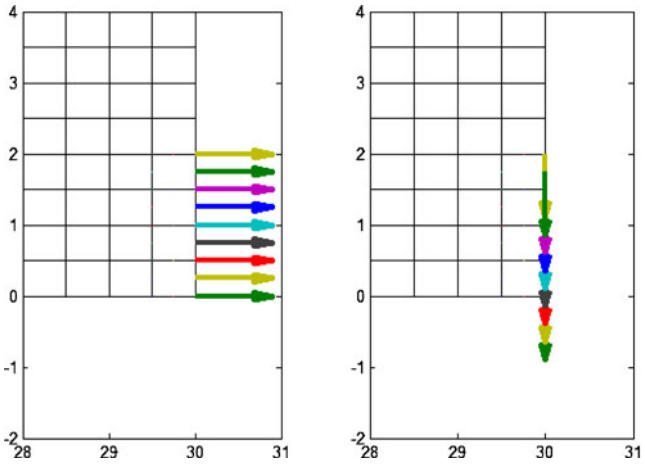

Fig. 9 Applied tension and bending loads at the bottom loading area of a cantilever beam

(Cherkaev and Cherkaev 2003). So we do not obtain the rank 2 designs with orthogonal laminates that appear in deterministic compliance optimization problems, cf. Allaire (2002). The nodal tractions, from which the surface traction is interpolated, corresponding to the worst-case load is shown in Fig. 6a. Note how the depicted worst-case loading differs from typical loadings, e.g. vertical bending load or tension load.

To illustrate that we have a consistent and convergent algorithm we repeat the optimization using a finer discretization, i.e. a 60×60 mesh, and as expected, we obtain a similar design (Fig. 7) and also a similar worst-case loading (Fig. 8a). The compliance values appear on Table 1.

To show the robustness of the design we compare the compliance value resulting from the worst-case loading to pure bending, tension and best-case loadings, cf. Table 1. The best-case loading, which corresponds to the smallest eigenvalue, yields an oscillatory high frequency loading that effectively cancels itself out in order to minimize the compliance, as depicted in Figs. 6b and 8b.[3] The pure tension and bending loadings are chosen such that they satisfy the norm constraint of (19), cf. Fig. 9. As seen in Table 1, the compliance converges with the mesh refinement for the pure bending and tension loads, but not for the best-case load, cf. footnote 3.

We emphasize that the structural displacement $\bar{\mathbf{u}}$ and therefore the worst-case loading $\mathbf{t}^*$ are scale multiples of the eigenvector $\mathbf{u}^{\max}$, i.e.,

$$\mathbf{t}^* = \frac{\bar{\mathbf{u}}}{\lambda_{\max}} = \alpha \frac{\mathbf{u}^{\max}}{\lambda_{\max}}, \tag{37}$$

[3] As mentioned in Cherkaev and Cherkaev (2003) the best-case loading problem is ill-posed. Indeed, the lowest eigenvalue (and hence best-case compliance) approaches, but never reaches zero.

Fig. 10 **a** "Second" Worst-case loading (corresponding to second largest eigenvalue) on the top and bottom loading areas

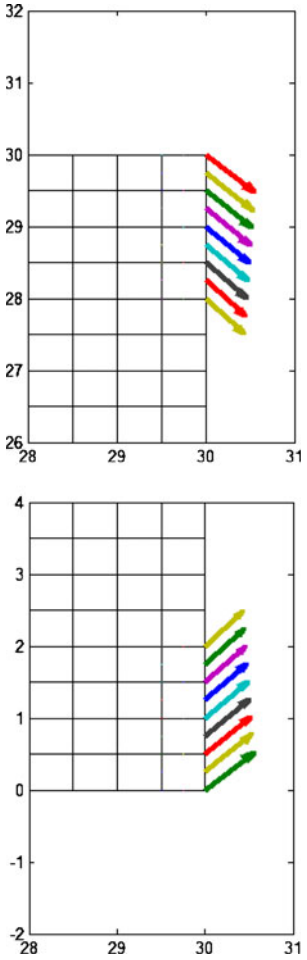

where α solves the load constraint of (34) and hence is written as

$$\alpha = \pm \frac{\bar{t}\,\lambda_{\max}}{\sqrt{(\int_{\Gamma_N} \mathbf{u}^{\max} \cdot \mathbf{u}^{\max}\, d\Gamma)}}. \tag{38}$$

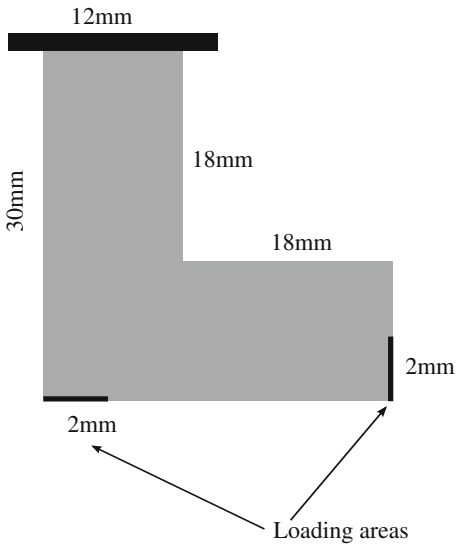

Fig. 11 L-bracket design space and loading areas

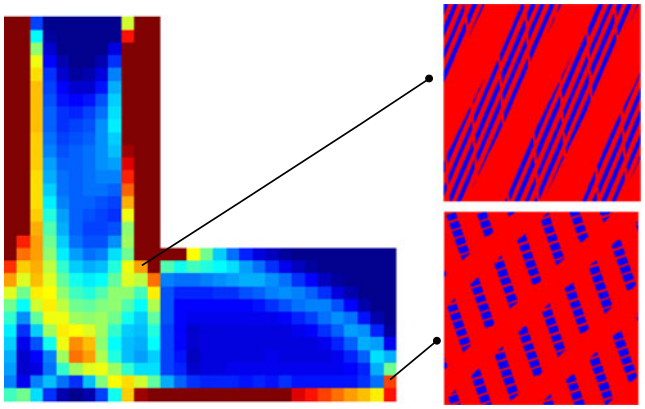

Fig. 12 Optimized L-bracket design (volume fraction ρ) for the minimum principal compliance problem obtained with the coarse mesh. The highlighted elements illustrate the ranked-laminate microstructure

In our numerical implementation, we used the positive value for α to evaluate the worst-case loading $\mathbf{t}^*$. However, the "mirror" worst-case loading $\mathbf{t}^*_M = -\mathbf{t}^*$ is also a solution which yields the same value for the principal compliance Λ. Note that the "mirror" worst-case loading $\mathbf{t}^*_M$ is not obtained due to a repeated maximum eigenvalue. Fortunately the maximum eigenvalues obtained in these examples are distinct. Figure 10 shows the second worst-case loading which is associated with the second largest eigenvalue and gives a compliance value equals to 0.87. If repeated eigenvalues are encountered, modifications must be made to the optimization algorithm, cf. Seyranian et al. (1994).

2.5.2 *L-bracket*

In the second example, we design an L-bracket subjected to two load areas, cf. Fig. 11. We show results for two different

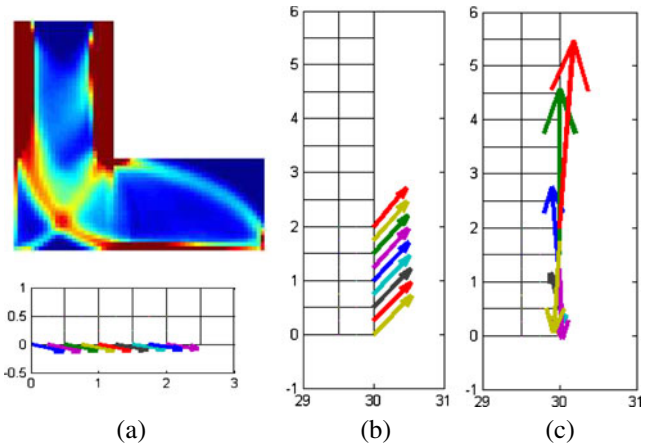

Fig. 13 Optimized L-bracket design (volume fraction ρ) for the minimum principal compliance problem obtained with the fine mesh. **a** Worst-case loading on the bottom loading area; **b** Worst-case loading on the right loading area; **c** Best-case loading on the right loading area

Table 2 Compliance comparison of L-bracket

Load case	Compliance (coarse mesh)	Compliance (fine mesh)
Worst-case	13.1555	12.9846
Best-case	.00181	.00051

mesh sizes: the coarse mesh has element size equals to 1 mm and the fine mesh has element size equals to 0.5 mm. Figure 12 shows the optimized design obtained with the coarse mesh. The finer discretization yields similar results, as shown on Fig. 13 and Table 2.

Figure 13 shows the worst-case loading and the best-case loading obtained with the fine mesh. Note that the best-case loading is concentrated on the right loading area and as in the first example, yields an oscillating behaviour that cancels itself out. The resulting compliance values for each loading appear in Table 2.

3 Conclusions

We have demonstrated an algorithm for robust design using topology optimization when the loading is unknown. The inner problem in the resulting minmax optimization formulation is solved directly by satisfying the optimality conditions which take the form of a Steklov eigenvalue problem and thereby we lessen the need for costly iterative nonlinear programming solvers.

Acknowledgments This work was funded by the US Army Research Office under MURI grant #W911NF-09-1-0436 (Dr. David Stepp program monitor).

Appendix

The weak formulation for the Steklov eigenvalue problem of (30) leads to the discretized residual

$$\prod_{e=1}^{\text{nel}} \int_{\Omega_e} \mathbf{G}^T \mathbb{C}^h \mathbf{G} \, d\Omega \, \boldsymbol{\phi}_e = \prod_{e=1}^{\text{nel}} \frac{1}{\lambda} \int_{\Gamma_{N_e}} \mathbf{N}^T \mathbf{N} \, d\Gamma \, \boldsymbol{\phi}_e \tag{39}$$

where $\prod$ is the element assembly process, $\mathbf{G}$ is the element strain-displacement matrix, $\mathbf{N}$ is the element shape function matrix and $\boldsymbol{\phi}_e$ is the element nodal eigenvector. The above reduces to

$$\mathbf{K}\boldsymbol{\phi} = \frac{1}{\lambda}\mathbf{M}\boldsymbol{\phi} \tag{40}$$

where $\mathbf{K}$ is the global stiffness matrix, $\mathbf{M}$ is the global distributed force matrix and $\boldsymbol{\phi}$ is the global nodal eigenvector. We solve the eigenvalue problem described in (40) for the maximum (reciprocal) eigenvalue, $\lambda_{\max}$, using a normalized power iteration. The corresponding eigenvector, $\boldsymbol{\phi}_{\max}$ may be subsequently scaled to obtain the corresponding displacement vector, cf. the discussion at the end of Section 2.4.1.

The sensitivities of the compliance are needed with respect to the ranked-laminate design parameters, cf. (26). Following Seyranian et al. (1994) we rearrange the eigenvalue equation as[4]

$$(\lambda\,\mathbf{K} - \mathbf{M})\boldsymbol{\phi} = \mathbf{0} \tag{41}$$

Differentiating the above with respect to a design variable, d_i, gives

$$\left(\frac{\partial\lambda}{\partial d_i}\mathbf{K}\right)\boldsymbol{\phi} + \left(\lambda\,\frac{\partial\mathbf{K}}{\partial d_i} - \frac{\partial\mathbf{M}}{\partial d_i}\right)\boldsymbol{\phi} + \left(\lambda\,\mathbf{K} - \mathbf{M}\right)\frac{\partial\boldsymbol{\phi}}{\partial d_i} = \mathbf{0} \tag{42}$$

where we note that the eigenvectors are scaled such that $\boldsymbol{\phi}^T\mathbf{K}\boldsymbol{\phi} = 1$. We now rearrange (42) and premultiply by the eigenvector, $\boldsymbol{\phi}$, to obtain

$$\frac{\partial\lambda}{\partial d_i} = -\boldsymbol{\phi}^T\left(\lambda\,\frac{\partial\mathbf{K}}{\partial d_i} - \frac{\partial\mathbf{M}}{\partial d_i}\right)\boldsymbol{\phi} \tag{43}$$

where we assume λ is a distinct eigenvalue and use the fact that $\boldsymbol{\phi}^T(\lambda\,\mathbf{K} - \mathbf{M})\frac{\partial\boldsymbol{\phi}}{\partial\mathbf{d}} = \frac{\partial\boldsymbol{\phi}}{\partial\mathbf{d}}^T(\lambda\,\mathbf{K} - \mathbf{M})\boldsymbol{\phi} = \mathbf{0}$ since $(\lambda, \boldsymbol{\phi})$ is an eigenpair. For our problem

$$\frac{\partial\mathbf{M}}{\partial d_i} = \mathbf{0} \tag{44}$$

and

$$\frac{\partial\mathbf{K}}{\partial d_i} = \prod_{i=1}^{\text{nel}}\int_{\Omega_e}\mathbf{G}^T\frac{\partial\mathbb{C}^h}{\partial d_i}\mathbf{G}\,d\Omega \tag{45}$$

where $\frac{\partial\mathbb{C}^h}{\partial d_i}$ is obtained from (11)–(18). Additional care must be taken if λ is a repeated eigenvalue, cf. Seyranian et al. (1994).

[4] Takezawa et al. (2011) reduce the size of this problem by using aggregation, but it is unclear if this is computationally advantageous. Indeed, we use SLEPc (Hernandez et al. 2005) to evaluate only the dominant eigenvalues; whereas the aggregation method requires an LU factorization of the stiffness matrix, multiple back substitutions, one for each force N node-direction combination and finally an eigenvalue analysis of a reduced $N \times N$ matrix.

References

Allaire G (2002) Shape optimization by the homogenization method. Springer-Verlag, New York

Allen M, Maute K (2005) Reliability-based shape optimization of structures undergoing fluid-structure interaction phenomena. Comput Methods Appl Mech Eng 194:3472–3495

Bendsøe M (1989) Optimal shape design as a material distribution problem. Struct Multidiscipl Optim 4:193–202

Bendsøe M, Sigmund O (2003) Topology optimization: theory, methods and applications. Springer-Verlag, Berlin

Bendsøe MP, Olhoff N, Taylor JE (1983) A variational formulation for multicriteria structural optimization. J Struct Mech 11(4):523–544

Chen S, Chen W, Sanghoon L (2010) Level set based robust shape and topology optimization under random field uncertainties. Struct Multidiscipl Optim 41:507–524

Cherkaev E, Cherkaev A (2003) Principal compliance and robust optimal design. J Elast 72:71–98

Cherkaev E, Cherkaev A (2008) Minimax optimization problem of structural design. Comput Struct 86:1426–1435

Conti S, Held H, Pach M, Rumpf M, Schultz R (2009) Shape optimization under uncertainty—a stochastic programming perspective. SIAM J Optim 19:1610–1632

Courant R, Hilbert D (1953) Methods of mathematical physics. Wiley, New York

Díaz A, Bendsøe M (1992) Shape optimization of structures for multiple loading conditions using a homogenization method. Struct Multidiscipl Optim 4:17–22

Díaz A, Sigmund O (1995) Checkerboard patterns in layout optimization. Struct Multidiscipl Optim 10:40–45

Du X, Sudjianto A, Chen W (2004) An integrated framework for optimization under uncertainty using inverse reliability strategy. J Mech Des 126:562–570

Gournay F, Allaire G, Jouve F (2008) Shape and topology optimization of the robust compliance via the level set method. COCV 14:43–70

Guest J, Igusa T (2008) Structural optimization under uncertain loads and nodal locations. Comput Methods Appl Mech Eng 198:116–124

Hernandez V, Roman JE, Vidal V (2005) SLEPc: A scalable and flexible toolkit for the solution of eigenvalue problems. ACM Trans Math S oftw 31(3):351–362

Jog C, Haber R (1996) Stability of finite element models for distributed-parameter optimization and topology design. Comput Methods Appl Mech Eng 130:203–226

Jung HS, Cho S (2004) Reliability-based topology optimization of geometrically nonlinear structures with loading and material uncertainties. Finite Elem Anal Des 41:311–331

Kharmanda G, Olhoff N, Mohamed A, Lemaire M (2004) Reliability-based topology optimization. Struct Multidiscipl Optim 26:295–307

Kogiso N, Ahn W, Nishiwaki S, Izui K, Yoshimura M (2008) Robust topology optimization for compliant mechanisms considering uncertainty of applied loads. J Adv Mech Des Syst Manu 2:96–107

Le C, Bruns T, Tortorelli D (2011) Material microstructure optimization for energy wave management. J Mech Phys Solids, to appear

Maute K, Frangopol D (2003) Reliability-based design of MEMS mechanisms by topology optimization. Comput Struct 81:813–824

Mozumder C, Patel N, Tillotson D, Renaud J (2006) An investigation of reliability-based topology optimization techniques. In: Proceedings of the 11th AIAA/ISSMO multidisciplinary analysis and optimization conference, AIAA, Portsmouth

Olhoff N (1989) Multicriterion structural optimization via bound formulation and matematical programming. Struct Optim 1:11–17

Park G, Lee T, Lee K, Hwang K (2006) Robust design: an overview. AIAA J 44(1):181–191

Seyranian A, Lund E, Olhoff N (1994) Multiple-eigenvalues in structural optimization problems. Struct Optim 8:207–227

Silva M, Tortorelli DA, Norato JA, Ha C, Bae H (2010) Component and system reliability-based topology optimization using a single-loop method. Struct Multidiscipl Optim 41:87–106

Sundaresan S, Ishii K, Houser D (1995) A robust optimization procedure with variations on design variables and constraints. Eng Optim 24:101–117

Svanberg K (1987) The method of moving asymptotes—a new method for structural optimization. Int J Numer Methods Eng 24(2):359–373

Takezawa A, Nii S, Kitamura M, Kogiso N (2011) Topology optimization for worst load conditions based on the eigenvalue analysis of an aggregated linear system. Comput Methods Appl Mech Eng 200:2268–2281

Tortorelli D, Michaleris P (1994) Design sensitivity analysis: overview and review. Inverse Probl Eng 1:71–105